



## **A geochemical overview of mid-Archaean metavolcanic rocks from southwest Greenland**

Szilas, Kristoffer

*Published in:*  
Geosciences (Switzerland)

*DOI:*  
[10.3390/geosciences8070266](https://doi.org/10.3390/geosciences8070266)

*Publication date:*  
2018

*Document version*  
Publisher's PDF, also known as Version of record

*Document license:*  
[CC BY](#)

*Citation for published version (APA):*  
Szilas, K. (2018). A geochemical overview of mid-Archaean metavolcanic rocks from southwest Greenland. *Geosciences (Switzerland)*, 8(7), [0266]. <https://doi.org/10.3390/geosciences8070266>

Review

# A Geochemical Overview of Mid-Archaean Metavolcanic Rocks from Southwest Greenland

Kristoffer Szilas 

Department of Natural Resource Management, University of Copenhagen, Øster Voldgade 10, 1350 Copenhagen, Denmark; krsz@ign.ku.dk; Tel.: +45-20816620

Received: 29 June 2018; Accepted: 16 July 2018; Published: 19 July 2018



**Abstract:** The present contribution reviews bulk-rock geochemical data for mid-Archaean (ca. 3075–2840 Ma) metavolcanic rocks from the North Atlantic Craton of southwest Greenland. The data set includes the most recent high quality major and trace element geochemical analyses for ten different supracrustal/greenstone belts in the region. When distilling the data set to only include the least altered metavolcanic rocks, by filtering out obviously altered samples, mafic/ultramafic cumulate rocks, late-stage intrusive sheets (dolerites) and migmatites, the remaining data ( $N = 427$ ) reveal two fundamentally distinct geochemical suites. The contrasting trends that emerge from the filtered geochemical data set, which best represents the melt compositions for these mid-Archaean metavolcanic rocks are: (1) tholeiitic (mainly basaltic) versus (2) calc-alkaline (mainly andesitic). These two rock suites are effectively separated by their La/Sm ratios (below or above three, respectively). It is demonstrated by geochemical modelling that the two contrasting suites cannot be related by either fractional crystallization or crustal assimilation processes, despite occurring within the same metavolcanic sequences. The tholeiitic basaltic rocks were directly mantle-derived, whereas the petrogenesis of the calc-alkaline andesitic rocks involve a significant (>50%) felsic component. The felsic contribution in the calc-alkaline suite could either represent slab-melt metasomatism of their mantle source, mafic-felsic magma mixing, or very large degrees of partial melting of mafic lower crust. At face value, the occurrence of andesites, and the negative Nb-Ta-Ti-anomalies of both suites, is consistent with a subduction zone setting for the origin of these metavolcanic rocks. However, the latter geochemical feature is inherent to processes involving crustal partial melts, and therefore independent lines of evidence are needed to substantiate the hypothesis that plate tectonic processes were already operating by the mid-Archaean.

**Keywords:** Archean; supracrustal belt; greenstone belt; geodynamics; andesite; magma-mixing

## 1. Introduction

Our understanding of the geodynamic environments that existed during the Archaean Eon is limited by a fragmented rock record for Earth's early history. Furthermore, ancient metavolcanic rocks are commonly affected by a range of modifying effects, including hydrothermal alteration, tectonic deformation, metamorphic overprint, and even melt loss [1,2]. In the present study, the Archaean record of metavolcanic rocks from southwest Greenland, part of the North Atlantic Craton, is examined with the aim of identifying their potential geodynamic setting(s) of formation.

Archaean tectonics is a contentious topic that has been debated for decades, and yet has not reached any consensus (see recent debate in other studies [3,4] and references therein). The erratic nature of the supracrustal belts of southwest Greenland (Figure 1) makes it difficult to gather large co-magmatic volcanic rock suites that can be used to determine their petrogenetic histories.

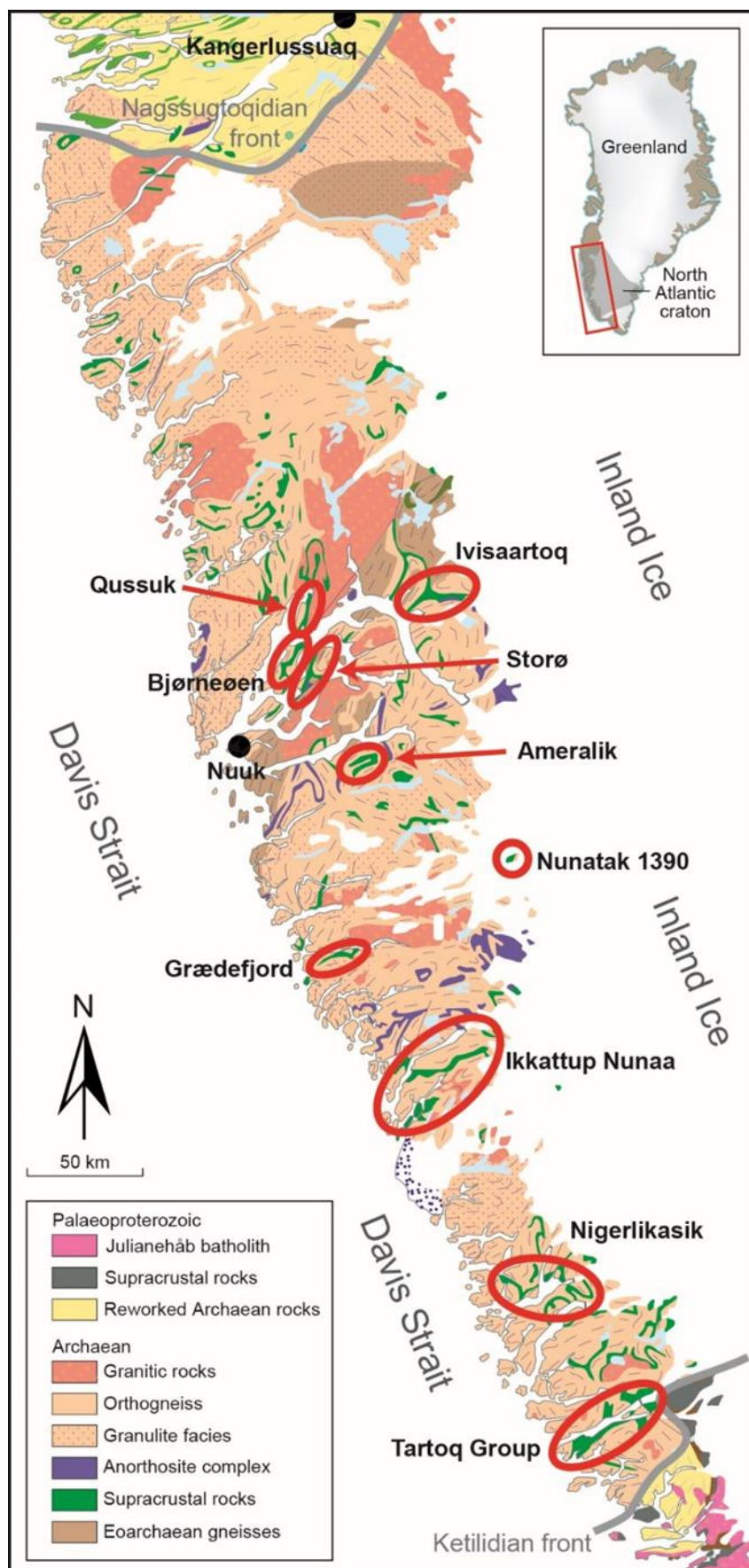


**Figure 1.** Geological map of the North Atlantic Craton of southern West Greenland. The red circles outline the areas that are discussed in the present review. Based on mapping by the Geological Survey of Denmark and Greenland (GEUS) [5].

These metavolcanic rocks occur as random inclusions and enclaves ranging in scales from decimeter to kilometer within the dioritic-tonalitic orthogneiss that comprises the continental crust of the North Atlantic Craton [5]. Systematic geological studies have been carried out on many individual metavolcanic rock suites in the region, and essentially all studies have concluded that they formed in a subduction zone-related setting [6,7]. However, this conclusion hinges on the negative Nb-Ta-Ti-anomalies observed in the geochemical data for the metavolcanic rocks, which resembles the trace element systematics of modern-style volcanic arc rocks [8].

The structural evolution also appears to support a horizontal tectonic regime during the Archaean Eon [7,9,10]. Finally, recent metamorphic modelling also points to pressure-temperature paths that are consistent with subduction zone settings [11,12]. Although the region has generally experienced amphibolite- to granulite-facies metamorphism, the geochemical composition of the metavolcanic belt have generally not been significantly affected, although there are areas which have indeed locally experienced melt loss and thus geochemical modification [2,6]. It is also important to point out that there appears to have been Eoarchaeon basement for at least some of the Mesoarchaeon supracrustal belts, as documented for the 3075 Ma Ivisartoq Supracrustal Belt [13]. However, this is likely to be the case only in the Nuuk region in association with the Eoarchaeon Itsaq Gneiss Complex (Figure 1).

In the present study the approach is to evaluate a geochemical database of Mesoarchaeon metavolcanic rocks, with the overall aim of investigating the large-scale petrogenetic variation. The samples range in age from 3075 Ma to 2840 Ma with no apparent geochemical differences with age. The main conclusion of the present study is that the mid-Archaean metavolcanic rocks of southwest Greenland fall in two discrete geochemical suites, which cannot be related by fractional crystallization and/or crustal assimilation processes.

The larger of the two groups is comprised of tholeiitic meta-basalts, which have essentially flat trace element patterns, and are typical of greenstone belts worldwide. The other group consists of calc-alkaline meta-andesites, which is a rock type that is far less common in Archaean cratons.

Geochemical modelling rules out simple assimilation of continental crust during the eruption of mafic magmas to produce the calc-alkaline andesitic suite. Instead it is a requirement of that its parental mantle-derived mafic magma mixed with a significant (>50%) felsic component, which could represent either: (1) slab-melt overprint of a mantle wedge, (2) large degrees of partial melting of mafic lower crust, or (3) moderate degrees of partial melting of continental crust.

Similar observations of rare andesitic rocks in other Archaean cratons have been made by other studies from China [14,15], Australia [16,17] and Canada [18,19]. Therefore, a better understanding of the petrogenesis of the mid-Archaean calc-alkaline andesites of southwest Greenland could have global implications and may thus lead to better constraints for Earth's early geodynamic settings.

## 2. Materials and Methods

A large geochemical data set ( $N > 500$ ) of well-characterized metavolcanic rocks was compiled from the most recent literature about the Archaean rock record of southwest Greenland. The compilation only includes rock suites for which modern high quality inductively coupled plasma mass spectrometry (ICP-MS) trace element data, as well as detailed field and petrographic observations are available. The data set was further constrained to only include supracrustal metavolcanic sequences.

Deep-seated layered complexes (e.g., Amikoq) and anorthosites (e.g., Fiskensæset) were not considered to avoid significant effects of fractional crystallization processes, and/or unusual parental magma compositions. For this reason, coarse gabbroic rocks were also excluded from the data compilation, even when they were associated with metavolcanic sequences, because such cumulate rocks are commonly affected by intercumulus liquid fractionation and the disproportionate accumulation of single minerals skew the geochemical composition of bulk-rock analyses [20].

It is important to point out that ultramafic rocks within the supracrustal sequences have major element compositions consistent with them representing cumulate portions of the metavolcanic

sequence that formed either as a consequence of in-situ crystal fractionation (olivine  $\pm$  pyroxene) in sills, or as magma conduits/feeder pipes for the associated volcanic sequence [21,22]. Such ultramafic rocks are commonly overprinted by alteration and metasomatism and now consist of serpentinite or amphibole-mica schist.

Because this review is concerned with the geochemical systematics of the metavolcanic rocks, and their implications for their geodynamic setting of formation, the ultramafic cumulate rocks were excluded from the final data set.

The above criteria for selection of samples resulted in a data set with a total of 436 bulk-rock analyses from the sources presented in Table 1 above. The metavolcanic data set was then subjected to minimal filtering, to avoid samples with obviously anomalous trace element patterns (e.g., extreme Zr-Hf-Ti-REE, high-field strength and rare earth elements, anomalies), which resulted in discarding nine samples (2% rejection rate). These anomalies can be both positive and negative and have no systematic trends. Some samples have one or more anomalies, but in all cases are interpreted at a “nugget effect” due to accessory minerals. The resulting data set that is investigated in the present study therefore includes 427 metavolcanic samples from ten different supracrustal belts across the North Atlantic Craton of southwest Greenland (Figure 1).

**Table 1.** Overview of the different literature sources of data used in the present review listed from north to south (see Figure 1). The full data compilation can be obtained upon request from the author.

| Supracrustal Belt/Greenstone Belt | Magmatic Age | Metavolcanic Samples (#) | References |
|-----------------------------------|--------------|--------------------------|------------|
| Ivisaartoq                        | 3075 Ma      | 54                       | [23–25]    |
| Qussuk                            | 3075 Ma      | 17                       | [26,27]    |
| Bjørneøen                         | 3075 Ma      | 11                       | [28]       |
| Storø                             | 2840 Ma      | 39                       | [29–31]    |
| Ameralik                          | ~3000 Ma     | 12                       | [32]       |
| Nunatak 1390                      | ~3000 Ma     | 29                       | [33]       |
| Grædefjord                        | 2975 Ma      | 35                       | [34]       |
| Ikkattup Nunaa                    | 2975 Ma      | 108                      | [35]       |
| Nigerlikasik                      | 2975 Ma      | 73                       | [36]       |
| Tartoq Group                      | >3000 Ma     | 58                       | [37]       |

It was found that the most effectively way to classify the metavolcanic rocks in distinct petrogenetic suites of tholeiitic and calc-alkaline affinity was to use their La/Sm ratio, which distinguishes a bimodal population within the data set as seen in Figure 2 above. The main argument for the robustness of this bimodal distribution is the fact that it occurs even on an outcrop scale, and that both geochemical suites display primary volcanic features, such as pillow structures and volcanoclastic features [23,26,27,35,36].

The geochemical freeware programme GCDKit [38] Version 5.0 was used to plot the data and trace element normalization values are also taken from this software.

Please note that I refer to the rocks interchangeably as tholeiitic basalt and melanocratic amphibolite, and calc-alkaline andesite and leucocratic amphibolite, respectively. Given that the entire region has undergone amphibolite- to granulite-facies metamorphism, and all rocks are metamorphic, the prefix “meta” is taken as being implicit for all lithological units described in the following. Also note that the term supracrustal belt is used for the metavolcanic belts of this region, and that this is equivalent with the term greenstone belt that is used in other cratons where the dominant metamorphic conditions are of greenschist-facies.



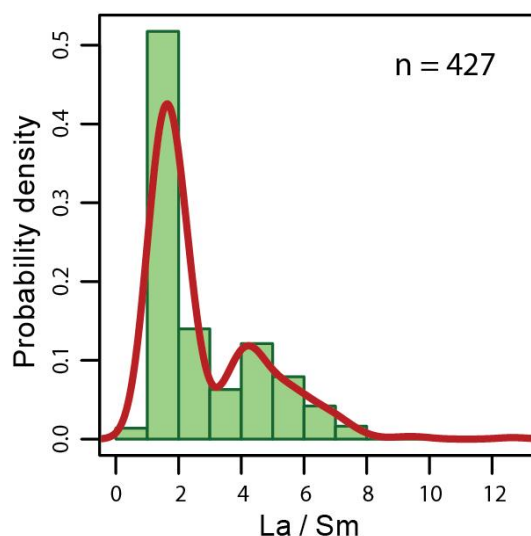


**Figure 2.** The basis for division in two distinct geochemical trends is a La/Sm ratio of below or above 3 for the tholeiitic and calc-alkaline suites respectively. The ratio is not normalized and uses the measured trace elements abundances.

### 3. Results

The geochemical database, which forms the basis of the present review, includes 427 metavolcanic samples of both tholeiitic ( $N = 287$ ) and calc-alkaline ( $N = 140$ ) affinity. To a first order, the mafic index of the rocks can be used as well, because the tholeiitic suite consists of mafic melanocratic amphibolites, whereas the calc-alkaline suite comprises intermediate leucocratic amphibolites, as a previous study pointed out [35]. However, as outlined in Figure 2 above, the data are bimodal in terms of their La/Sm, which is a ratio that effectively separates the metavolcanic rocks in the two discrete suites. In the following, the main geochemical features of the two metavolcanic suites are outlined.

#### 3.1. Tholeiitic Basalts

The melanocratic amphibolites have La/Sm ratios below 3 with an average of 1.7 (Appendix A, Figure A1), and are therefore classified as the Low La/Sm group throughout this work. These rocks follow a tholeiitic fraction trend as seen in Figure 3 below, which is also the case in other types of discrimination diagrams (Appendix A, Figure A2). This suite is basaltic with an average  $\text{SiO}_2$  of 50.9 wt % (Appendix A, Figure A3a), which is also observed when only considering immobile element ratios for a more robust classification of metavolcanic rocks (Figure 4).

The tholeiitic basaltic suite is metaluminous with an average  $\text{Al}_2\text{O}_3$  of 14.8 wt % (Figure 5), but with significantly higher average  $\text{Na}_2\text{O}$  (2.1 wt %) than  $\text{K}_2\text{O}$  (0.3 wt %). The average CaO contents is 10.8 wt % consistent with the large modal abundance of plagioclase in these rocks. The average  $\text{TiO}_2$  contents of the tholeiitic Low La/Sm group is 1.1 wt % with a total range from 0.3 to 3.0 wt %.

The Low La/Sm group has an average MgO of 7.4 wt %, however as can be seen in Figure 5, there is a sub-group with slightly higher MgO clustering at around 15 wt %. Please note that this data set has been filtered for apparent gabbroic and ultramafic cumulate rocks (see Section 2), although this step inherently relies on the rock descriptions found in the literature. Total FeO averages 12.4, with a range from 5.6 to 19.7 wt %. The broad range in  $\text{FeO}^T$  and MgO results in an equally wide bulk-rock Mg# from around 75 to 30 as seen in Figure 6.

The primitive mantle-normalized trace element diagram for the tholeiitic Low La/Sm group is rather flat, consistent with the average La/Sm ratio of 1.7 (Figure 7). However, there are subtle negative Nb-Ta-Ti-anomalies, and obvious positive anomalies for U and Pb.

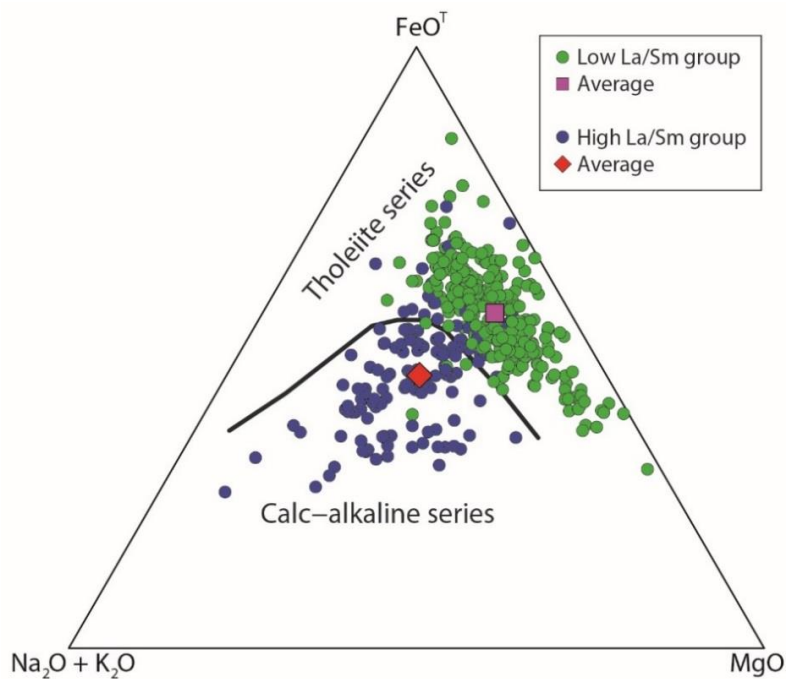


**Figure 3.** AFM diagram [39] showing the tholeiitic fractionation trend of the basalts, in contrast to the mainly calc-alkaline trend of the andesites.

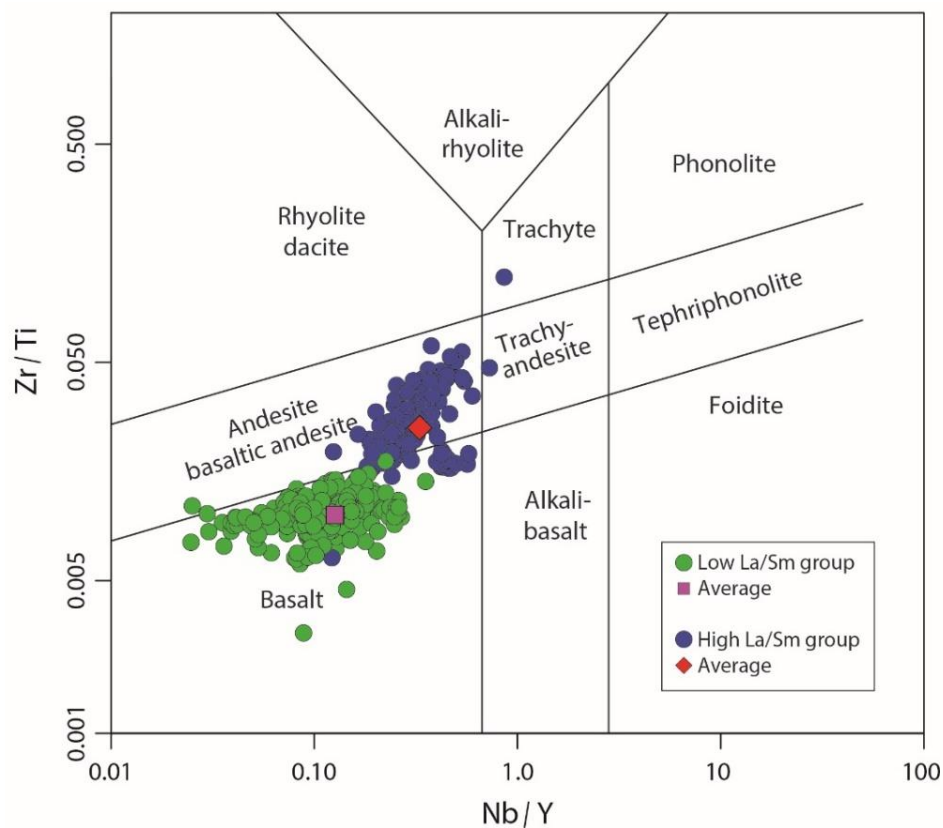


**Figure 4.** Classification diagram for volcanic rocks that rely on fluid immobile element ratios [40], which is also applicable to metamorphic rocks. The two metavolcanic suites display distinct populations in this diagram, where the Low La/Sm tholeiitic group is basaltic, and the High La/Sm calc-alkaline group is main basaltic andesite to andesite.

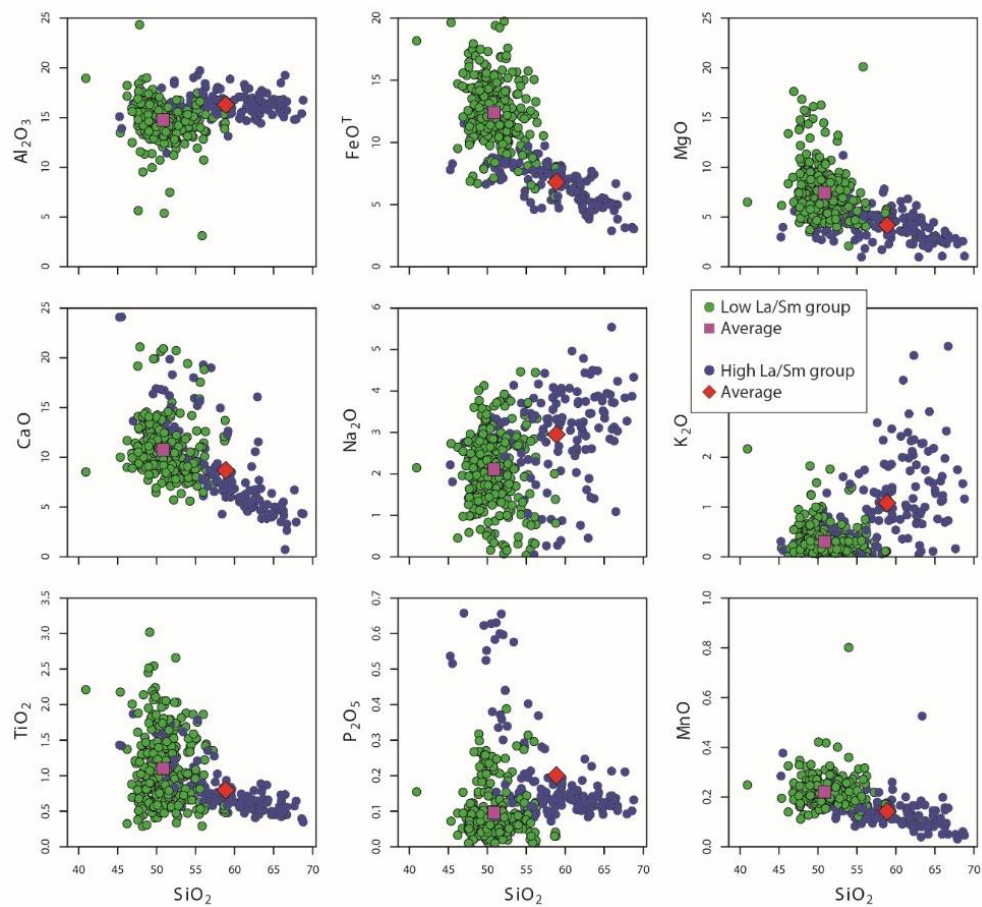


**Figure 5.** Major elements plotted against  $\text{SiO}_2$  content. At face value, the two metavolcanic suites appear to represent a continuum that could potentially be related by fractional crystallization. However, such a relationship is incompatible with their range in Mg# (Figure 6), as well as with the discrete trace element groups (Figure 7).

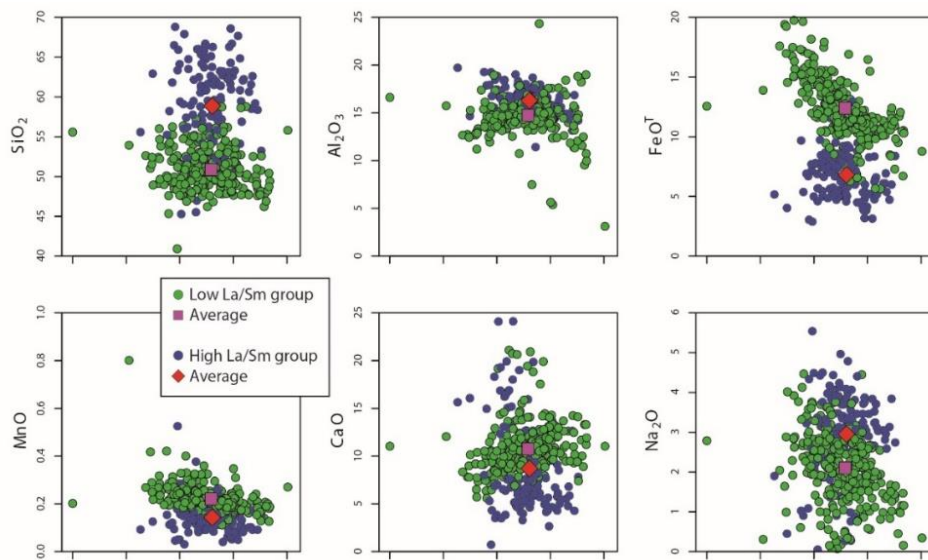


**Figure 6.** Cont.



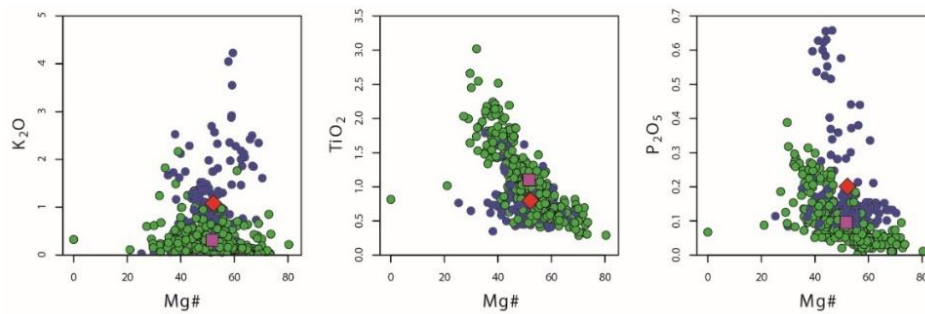


**Figure 6.** Major elements plotted against Mg#, which is calculated as the atomic proportions of  $\text{MgO}/(\text{MgO} + \text{FeO}^{\text{T}})$ . Note the overlapping ranges of Mg# for the two suites, which is inconsistent with a relationship between the basalts and andesites by fractional crystallization processes.

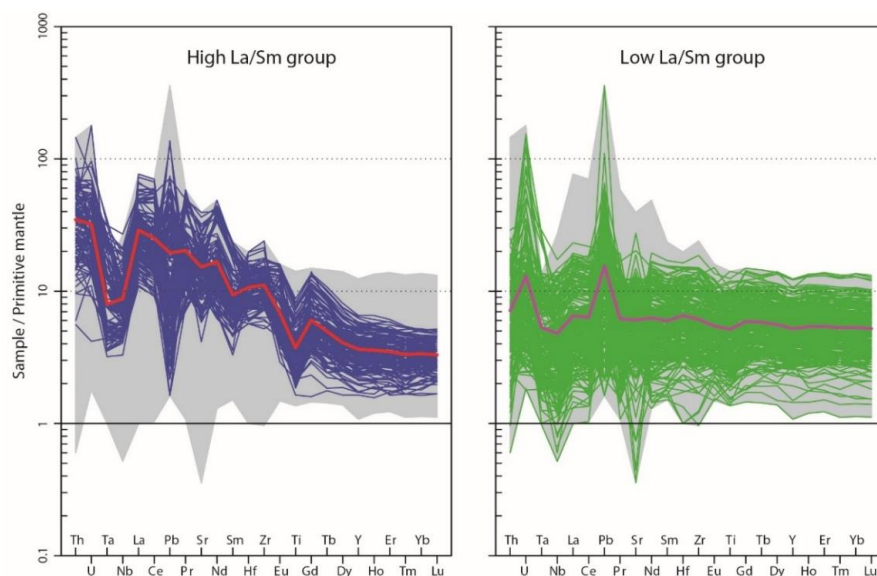


**Figure 7.** Primitive mantle-normalized trace element diagram for the two groups of metavolcanic rocks. Note the negative Nb-Ta-Ti-anomalies in both suites. Normalization values from reference [41].

### 3.2. Calc-Alkaline Andesites

The leucocratic amphibolites mostly have La/Sm ratios above 3 with an average of 5.1. (Appendix A, Figure A1). They follow a distinct calc-alkaline fractionation trend, as seen in Figures 3 and A2. For simplicity, the High La/Sm group of intermediate rocks are here referred to as calc-alkaline andesites, although they have  $\text{SiO}_2$  ranging from 45.3 to 68.8 wt %, and thus technically classify as basaltic to dacitic with a mean value of an andesitic composition (Appendix A, Figure A3a). However, this nomenclature appears reasonable despite the range of  $\text{SiO}_2$  (Figure 5). This is seen in Figure 3, which is a diagram that only relies on fluid immobile element ratios, rather than  $\text{SiO}_2$ , and is therefore far less susceptible to disturbance during metamorphic processes.

Figures 3 and A2, clearly demonstrates the calc-alkaline affinity of the High La/Sm group. These calc-alkaline andesites are also characterized by a wide range of CaO (0.7–24.1 wt %),  $\text{Na}_2\text{O}$  (0.1–5.5 wt %), and  $\text{K}_2\text{O}$  (0.0–4.2 wt %), as seen in Figure 5. A subset of the andesites are peraluminous (Figure A3b).

The calc-alkaline andesitic suite has systematically lower  $\text{FeO}^{\text{T}}$  (average of 6.8 wt %) and MgO (average of 4.2 wt %) than the tholeiitic basaltic suite (Figure 5). Nevertheless, the High La/Sm group covers essentially the same range of bulk-rock Mg# from 40 to 70 (Figure 6).

The primitive mantle-normalized trace element diagram of the calc-alkaline andesitic suite shows enriched patterns with a negative slope. The combination of negative Ta-Nb-Ti-anomalies with otherwise continuous enrichment resembles typical crustal rocks in continental settings. Some of the andesites have positive Zr-Hf-anomalies, and others have negative Sr-anomaly, whereas Pb can be both positive or negative (Figure 7).

Although the andesites generally have high abundances of the incompatible elements (Figure A4), it is worth noting that the High La/Sm group has relatively low Y and heavy rare earth elements (HREE) in comparison with the Low La/Sm group (Figures 7 and A1). The andesites have lower abundances of compatible trace elements, despite the general overlap in bulk-rock Mg# (Figure A4).

The calc-alkaline andesitic suite has systematically lower  $\text{FeO}^T$  (average of 6.8 wt %) and MgO (average of 4.2 wt %) than the tholeiitic basaltic suite (Figure 5). Nevertheless, the High La/Sm group covers essentially the same range of bulk-rock Mg# from 70 to 40 (Figure 6).

The primitive mantle-normalized trace element diagram of the calc-alkaline andesitic suite shows enriched patterns with a negative slope. The combination of negative Ta-Nb-Ti-anomalies with otherwise continuous enrichment resembles typical crustal rocks in continental settings. Some of the andesites have positive Zr-Hf-anomalies, and others have negative Sr-anomaly, whereas Pb can be both positive or negative (Figure 7).

Although the andesites generally have high abundances of the incompatible elements (Appendix A, Figure A4), it is worth noting that the High La/Sm group has relatively low Y and HREE in comparison with the Low La/Sm group (Figures 7 and A1). The andesites have lower abundances of compatible trace elements, despite the general overlap in bulk-rock Mg# (Figure A4).

#### 4. Discussion

The observation that the supracrustal belts of southwest Greenland hosts two distinct metavolcanic suites is important for the understanding of their geodynamic setting(s). As emphasized at the outset, the La/Sm ratio is effective at separating the metavolcanic sequence in two distinct suites, with minimal overlap also as seen in Figure 8 below.

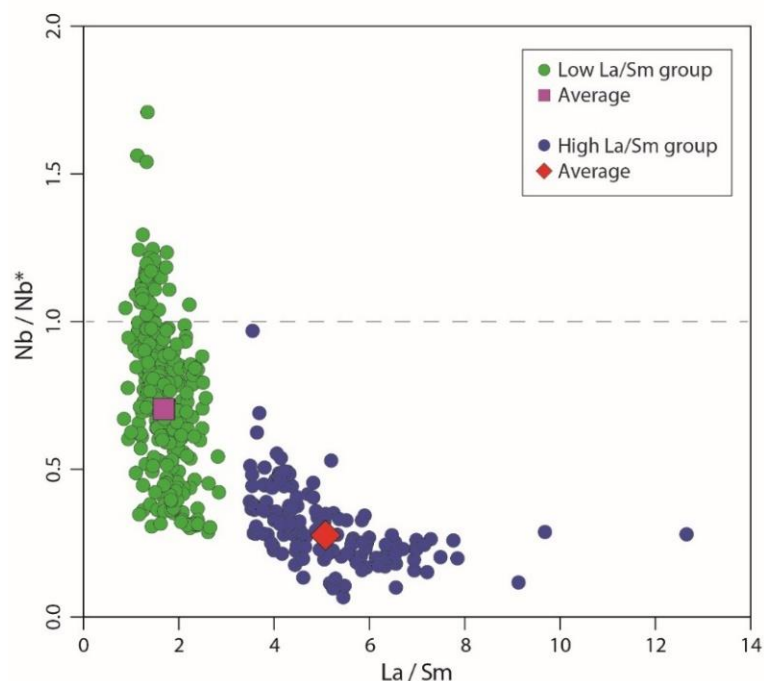


**Figure 8.** Plot of Nb-anomaly calculated as  $\text{Nb}/\text{Nb}^* = \text{Nb}_N / \sqrt{(\text{Th}_N \cdot \text{La}_N)}$  against La/Sm. ‘N’ denotes normalization to primitive mantle abundances (see Figure 7).

The rocks of the tholeiitic basaltic suite (Low La/Sm group) have geochemical compositions typical of Archean basalts with overall flat trace element patterns, negative Nb-anomalies (Figure 8), and relatively high Ni, Cr and Co [42,43]. These features are consistent with an origin by decompression melting of primitive mantle, potentially with the influence of fluids to account for the stability of a residual phase that can accommodate Nb [44]. The high MgO rocks plot in the mid-range in terms of Nb-anomalies and there appears to be no systematic trend between MgO and Nb/Nb\* within the basaltic metavolcanic group.

The calc-alkaline andesites (High La/Sm group) have enriched incompatible trace element compositions with negative Nb-Ta-Ti-anomalies that are typical features of arc-related rocks [45]. However, the fact that the andesitic rocks have overall lower abundances of the HREE (Figure 7), as well as Y (Appendix A, Figure A4), indicates that garnet was present in their residual source region [46], as also pointed out in a previous study [36].

Andesites are commonly associated with subduction zone settings, although their petrogenesis is somewhat ambiguous with interpretations ranging from them representing fractional crystallization products of initial basaltic mantle-derived magmas [47], direct melts of metasomatized mantle [48], or result of bimodal magma mixing [49]. Although geotectonic discrimination diagrams have essentially been abandoned [50], they still serve a purpose to distinguish rock suites with geochemical features that are characteristic of crustal settings and/or crustal contamination, as seen in Figures 9 and 10 on the next page. The tholeiitic basalts plot in regions typical of mid-ocean ridge basalts (MORB) or oceanic island arcs, whereas the calc-alkaline andesites plot as continental or alkaline arcs.

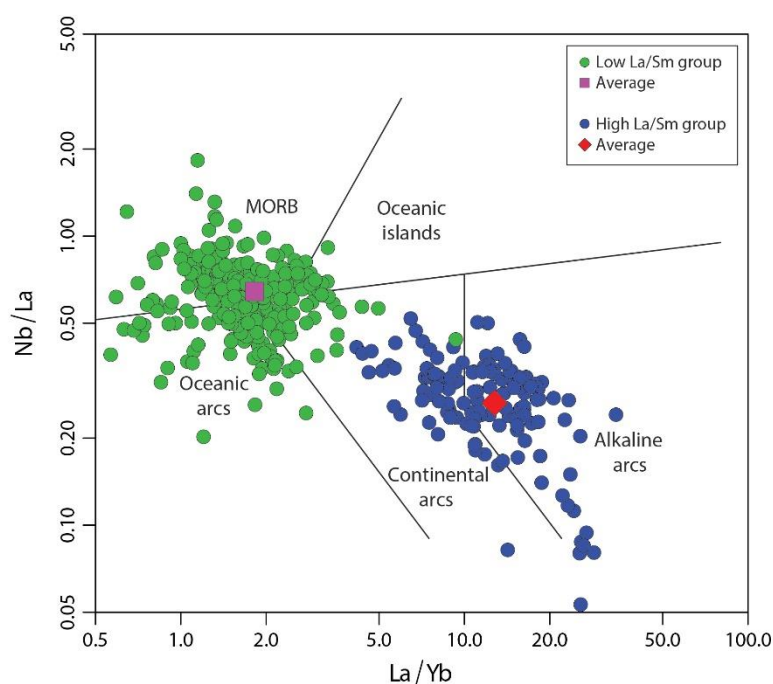


**Figure 9.** Tectonic discrimination diagram [51] demonstrating the bimodality of the metavolcanic rocks of southwest Greenland. Figure A5 also displays similar distinct trace element systematics. Abbreviations: MORB = mid-ocean ridge basalts.

In these diagrams the two metavolcanic rock suites are almost completely separated with minimal overlap, which is incompatible with them having a relationship by simple crystal fractionation. This is also obvious when considering the bulk-rock Mg#-trends of Figure 6, where the andesites have values up to about 70, and could thus potentially represent direct mantle melts [48].

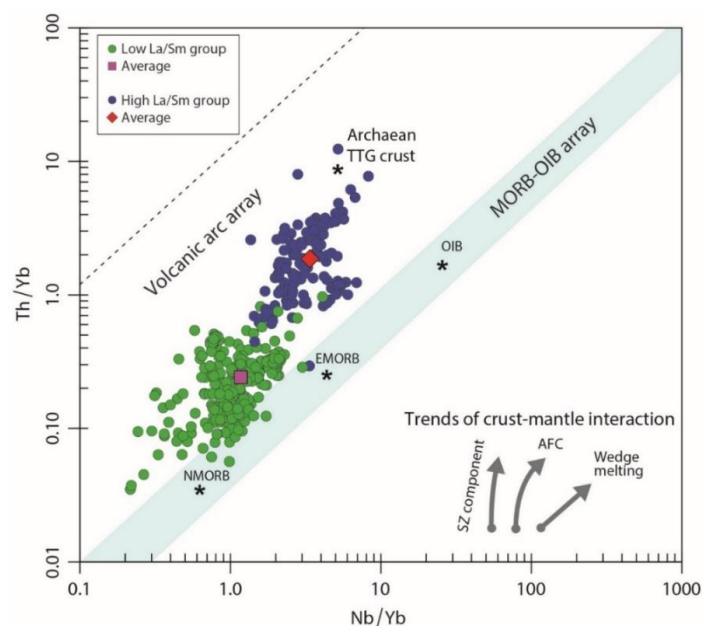


**Figure 10.** Pearce discrimination diagram showing various mantle reservoirs and vectors of crust-mantle interaction [52]. Archaean TTG crust (asterisk symbol) is shown for reference as a potential contaminant for the metavolcanic rocks. Abbreviations: TTG = tonalite-trondhjemite-granodiorite; OIB = oceanic island basalts; SZ = subduction zone component; AFC = assimilation during fractional crystallization.

Figure 11 below shows trace element modelling of the effects of fractional crystallization (FC), assimilation during fractional crystallization (AFC), and magma mixing, respectively. The modelling parameters were taken from a recent study of the Qussuk Supracrustal Belt [27]. The local average Archaean tonalite-trondhjemite-granodiorite (TTG) crust was used as the contaminant and felsic mixing end-member, and an R-factor of 0.3 was used. A primitive basalt (sample 477378) was applied as a potential parental melt composition. For simplicity, the steps for each model are not shown, but only the overall trend lines to demonstrate the effects of the different processes.

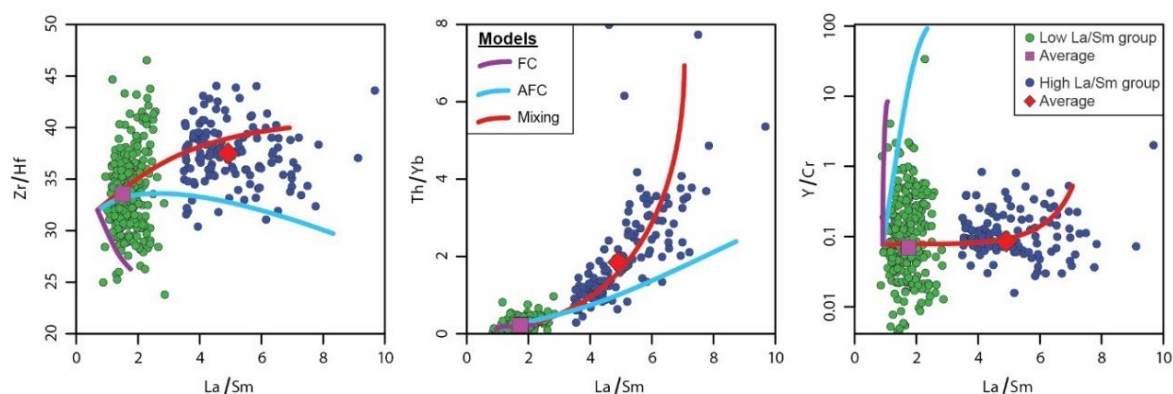


**Figure 11.** Trace element modelling of fractional crystallization (FC), assimilation during fractional crystallization (AFC), and magma mixing (Mixing).

The main observation of the FC model is that the variation within the Low La/Sm tholeiitic suite can be adequately explained by simple crystal fractionation using equal proportions of olivine, clinopyroxene and plagioclase. This is consistent with the systematic trends of both major and trace

elements, when plotted against bulk-rock Mg# (Figures 6 and A4), as well as the minimal change in La/Sm ratio within this group.

The AFC model shows the effect of TTG-type crust assimilation in a mafic parental melt, as would be expected during eruption of tholeiitic basalts through Archaean continental crust. This effect has been proposed as an explanation for the general offset of Archaean basalts from the mantle array typically seen in Pearce Diagrams as the one in Figure 10 [53]. However, the data for calc-alkaline andesitic rocks from southwest Greenland presented in this study cannot be explained by AFC processes involving continental crust, because the trajectories are offset from the majority of the samples, including the average composition. It would simply require an unrealistically high R-factor and would effectively mean that the crustal assimilant was dominating the system, which is not consistent with thermal conditions controlled by the latest heat of crystallization [54].

Instead, a model involving large degrees of magma mixing of a mafic and a felsic endmember, seems to be the best of the three trace element models presented in Figure 11 above. This is also consistent with the bimodal trace element systematics observed in Figures 9 and 10, as well as the continuous SiO<sub>2</sub> variation seen in Figure 5, which seems to be converging at a felsic endmember.

Several recent studies of modern andesites including comprehensive melt inclusion measurements [49,55], indicate that such intermediate compositions can indeed form as a result of melt mixing in deep-seated magma chambers with homogenization to form andesitic melts prior to the eruption of arc lavas.

Interestingly, although the geochemical systematics of the andesites strongly support a petrogenesis involving magma mixing between mafic and felsic endmembers, a modern-style subduction zone origin for the Archaean andesites is not necessarily needed. One recent study proposed that such rocks represents mixing of mantle-derived mafic melts with high-pressure (garnet-bearing) anatectic melts within complex plumbing system [56]. Yet another study argued for the involvement of komatiitic melt contaminated by TTG-type dacite in petrogenesis of mid-Archaean andesites from the Yilgarn Craton of Australia [57]. Therefore, one outcome of the present review is that geochemical data alone is not sufficient by itself to determining the geodynamic setting of Archaean metavolcanic rocks. Several lines of evidence are needed, including detailed field observations, structural studies, and metamorphic P-T-t modelling.

One entirely different way to form the observed trace element systematics of discrete basaltic and andesitic rocks would be if there was mechanical mixture of tholeiitic metavolcanic rocks with tonalitic continental crust. However, in that case one would expect significant alteration of the mixed product due to associated fluid migration in thrust zones. This is not seen when plotting the data in a weathering plot as seen in Figure A6, which would also highlight altered samples. Although the andesites have the highest W-index samples ( $W = \text{weathering}$ ), the vast majority plots right on the igneous fractionation line, which is inconsistent with them being significantly altered. Nevertheless, a model of tectonic intercalation should be kept in mind for the origin of similar andesites, due to the structurally complex and poly-metamorphic history of many Archaean cratons.

Future work on the petrogenesis of the mid-Archaean metavolcanic rocks of southwest Greenland (or global occurrences) could focus on testing one or several of the following hypotheses, which would help rejecting some of current models:

- Leucocratic amphibolites of intermediate composition (andesites) represent melts derived from slab-melt metasomatized mantle wedge [48]. This process would be an analogue for subduction zone processes found at modern-style island arcs.
- The andesites represent mixing/homogenization of juvenile mafic magmas with felsic partial melts derived from lower crust of either mafic or felsic composition in deep-seated magma chambers that underwent subsequent fractional crystallization of plagioclase + clinopyroxene  $\pm$  garnet. This process would be an analogue for modern-style andesite formation along continental margins, although non-uniformitarian scenarios have also been proposed [56,57].



- The andesites formed by large degree melting of the same mafic source as the regional TTG-suite orthogneiss. In this case the andesites would therefore represent an early stage volcanic equivalent to the regional granitoid crust, which would explain their common hafnium-isotopic features.
- Finally, the andesites formed by tectonic intercalation of mafic metavolcanic rocks and younger TTG-suite continental crust, and thus simply represents a mechanical mixture. This case would negate any previous study of the andesites, which interprets these rocks in a context volcanic processes with implications on geodynamic settings. Detailed field and structural observations would be essential for testing this latter tectonic intercalation model.

In all the above hypotheses, bulk-rock Sm-Nd and Lu-Hf isotopes in combination with zircon in situ Hf-isotopes would serve as important tools for constraining the involved geochemical reservoirs. Modern methods of integrated metamorphic pseudo-section and trace element geochemical modelling would be instrumental in discriminating between the different scenarios outlined above. However, underlying detailed field observations and structural studies are of vital importance when assessing ancient rocks, such as those of the Archaean cratons worldwide.

## 5. Conclusions

The main result of the present study of the geochemical database for mid-Archaean metavolcanic rocks from southwest Greenland, is the occurrence of two fundamentally distinct petrogenetic suites, namely: (1) tholeiitic basalts versus (2) calc-alkaline andesites.

The tholeiitic basalts consistently have flat/unfractionated patterns with subtle negative anomalies for Nb-Ta-Ti on primitive mantle-normalized trace element diagrams. The calc-alkaline metavolcanic rocks on the other hand, display steep/fractionated trace element patterns in combination with even stronger negative Nb-Ta-Ti-anomalies, and thus point to a strong crustal affinity.

Trace element modelling can be used to reject models involving simple fractional crystallization or crustal assimilation as a means of relating the petrogenesis of the andesites from a basaltic parental melt. Instead it is a requirement that the andesites formed in a process that involves significant mixing of mafic and felsic endmember magmas. However, from geochemical data alone it is not possible to demonstrate in which geodynamic setting such andesites formed.

Future work on Archaean andesites should integrate several lines of evidence, including field, structural and metamorphic studies to reject some of the competing petrogenetic models.

**Author Contributions:** The author carried out the present review independently, based on existing geochemical data published in the literature. Please contact the author to obtain the compiled data set used in the present study.

**Funding:** This review was made possible by support from VILLUM FONDEN through grant number 18978. The Article Processing Charges (APC) were generously waived by MDPI.

**Acknowledgments:** The author would like to thank his many colleagues and collaborators for many fruitful discussions and much useful insights gained over the past ten years on the subject of Archaean metavolcanic rocks from Greenland. The contributors are too many to list here, but without them we would not have access to the data presented in this study. Two anonymous reviewers are acknowledged for constructive comments.

**Conflicts of Interest:** The author declares no conflict of interest. The funders had no role in the design of the study; in the collection, analyses, or interpretation of data; in the writing of the manuscript, or in the decision to publish the results.

## Appendix

Below are given several supplementary diagrams to further illustrate the main geochemical differences between the two metavolcanic suites of southwest Greenland, which can be divided into a tholeiitic basaltic suite and a calc-alkaline andesitic suite based on their La/Sm ratios:

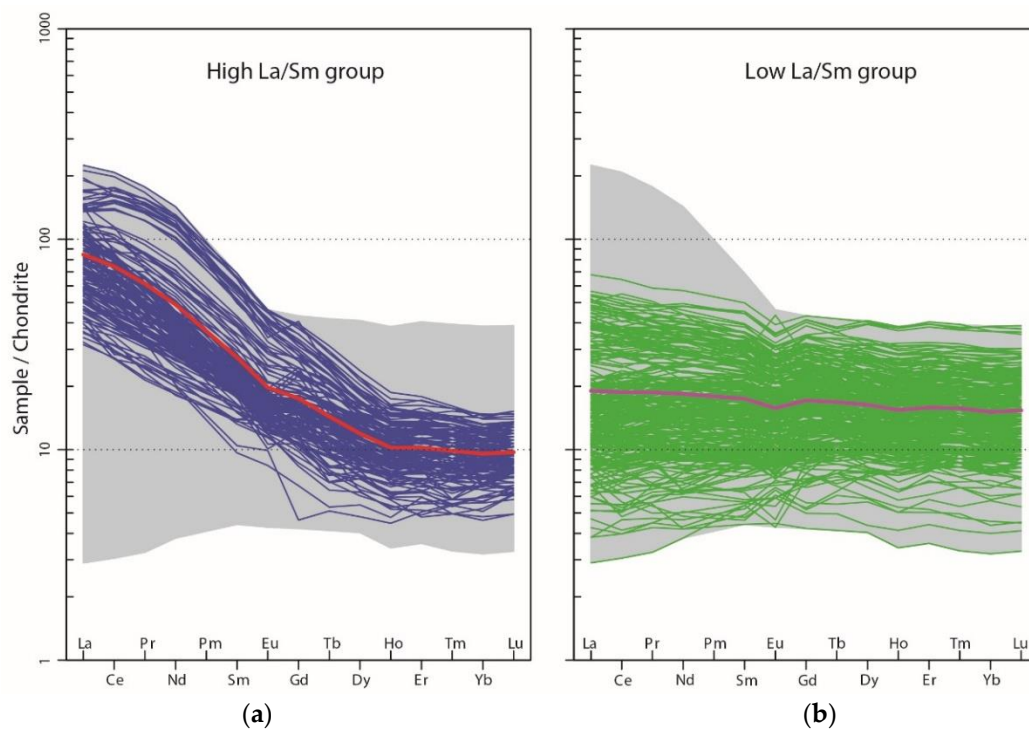


**Figure A1.** Rare Earth Element (REE) diagram for the two groups of metavolcanic rocks. Normalization to chondrite from [58]. (a) High La/Sm calc-alkaline andesites; (b) Low La/Sm tholeiitic basalts. Both groups have dominantly mild negative Eu-anomalies with averages around 0.9.

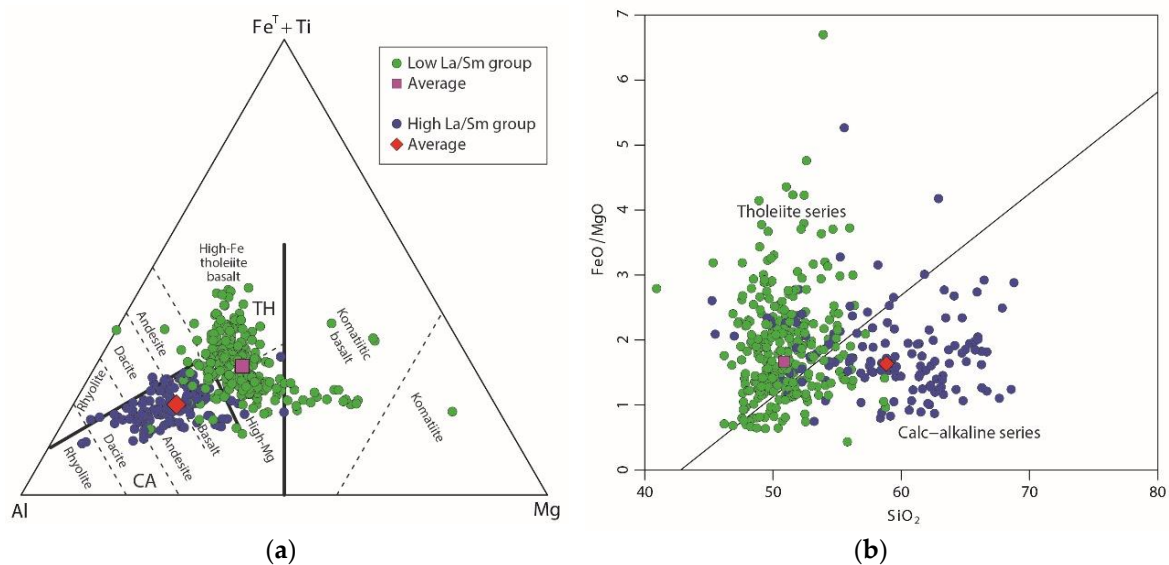


**Figure A2.** (a) Jensen diagram [59] showing that the average compositions of the two metavolcanic suites are tholeiitic basalts and calc-alkaline andesites, respectively; (b) Miyashiro diagram showing that the two metavolcanic suites are broadly tholeiitic and calc-alkaline [60]. CA = calc-alkaline; TH = tholeiitic.

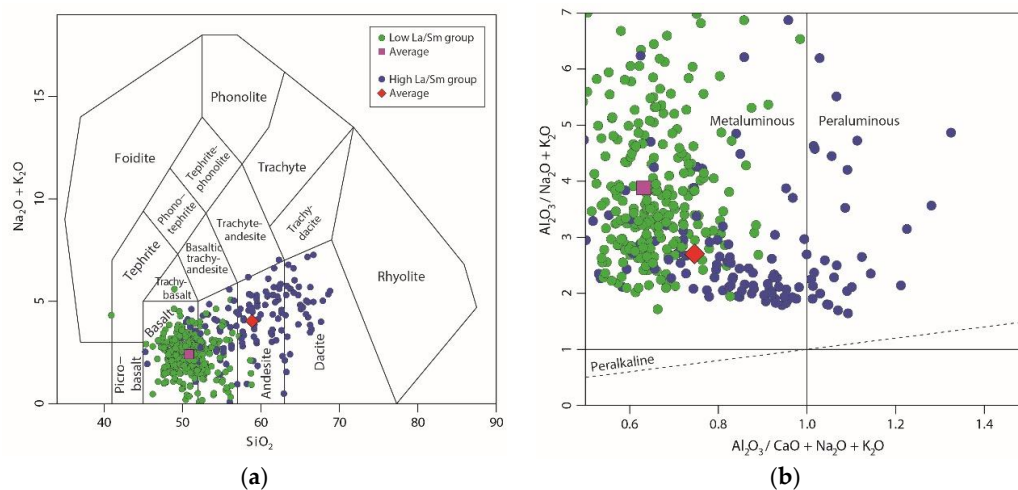


**Figure A3.** (a) TAS classification diagram [61] showing that the average tholeiite suite is basaltic, whereas the average calc-alkaline suite is andesitic; (b) Classification diagram that discriminates metaluminous, peraluminous and peralkaline compositions [62].

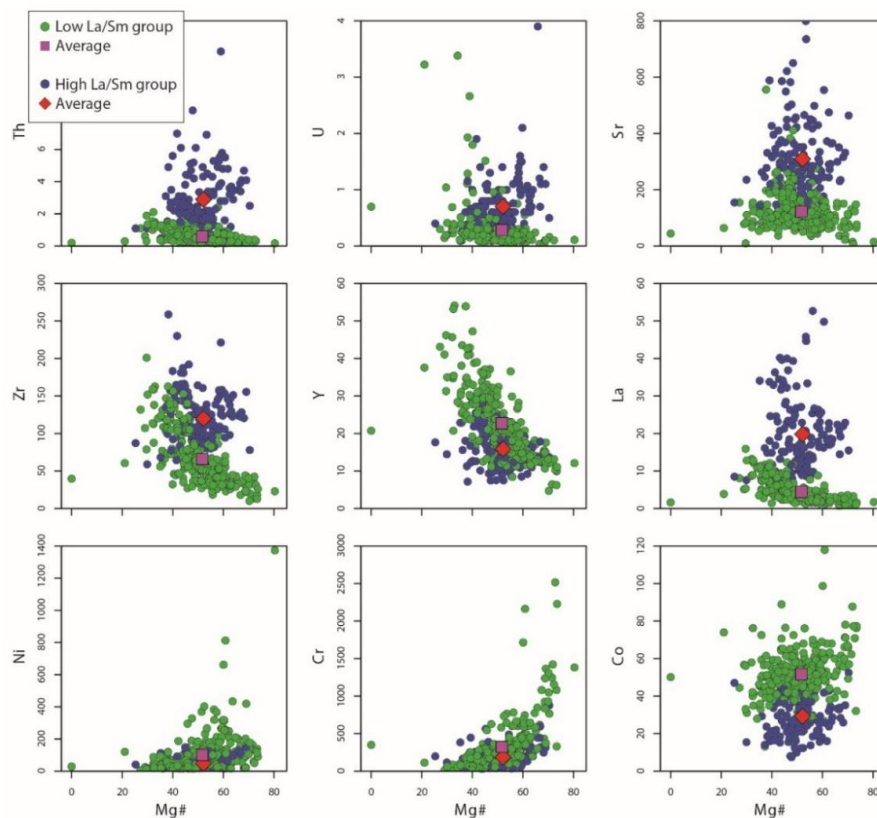


**Figure A4.** Trace element abundances (ppm) plotted against bulk-rock  $\text{Mg\#}$  (atomic  $\text{Mg}/[\text{Mg} + \text{Fe}^{\text{Total}}]$ ) of the two metavolcanic suites. The incompatible trace element concentrations are generally elevated for the calc-alkaline high La/Sm rocks apart from Y (and Heavy Rare Earth Elements (HREE)). The latter may indicate garnet in their source region. The compatible trace elements are generally higher in the tholeiitic suite.

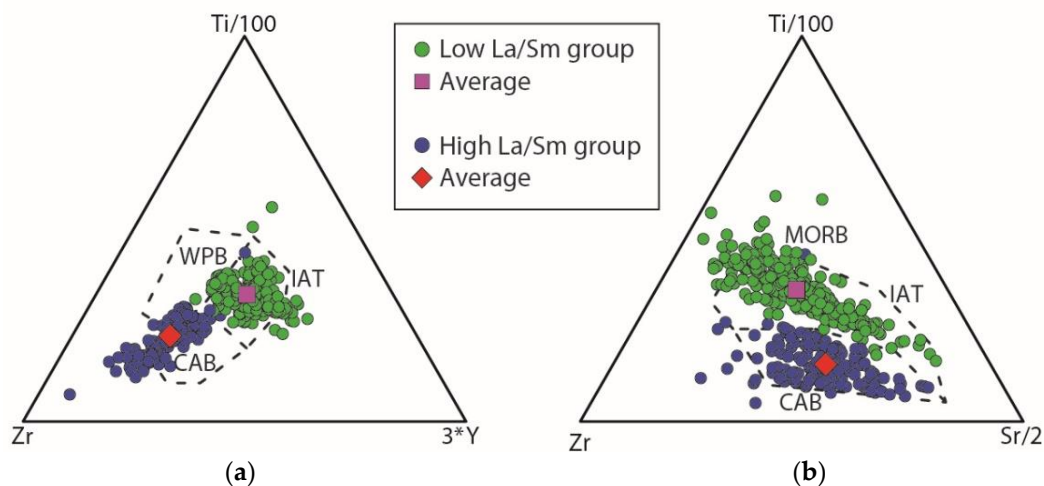


**Figure A5.** Tectonic discrimination diagrams with (a) Zr, Ti/100, 3\*Y, (b) Zr, Ti/100, Sr/2 [63], showing the two discrete populations within the metavolcanic data set. The tholeiitic suite consistently plots in the mid-ocean ridge basalt (MORB) or island arc tholeiite (IAT) fields, whereas the calc-alkaline suite always plots as continental arc basalts (CAB). WPB = within-plate basalts.

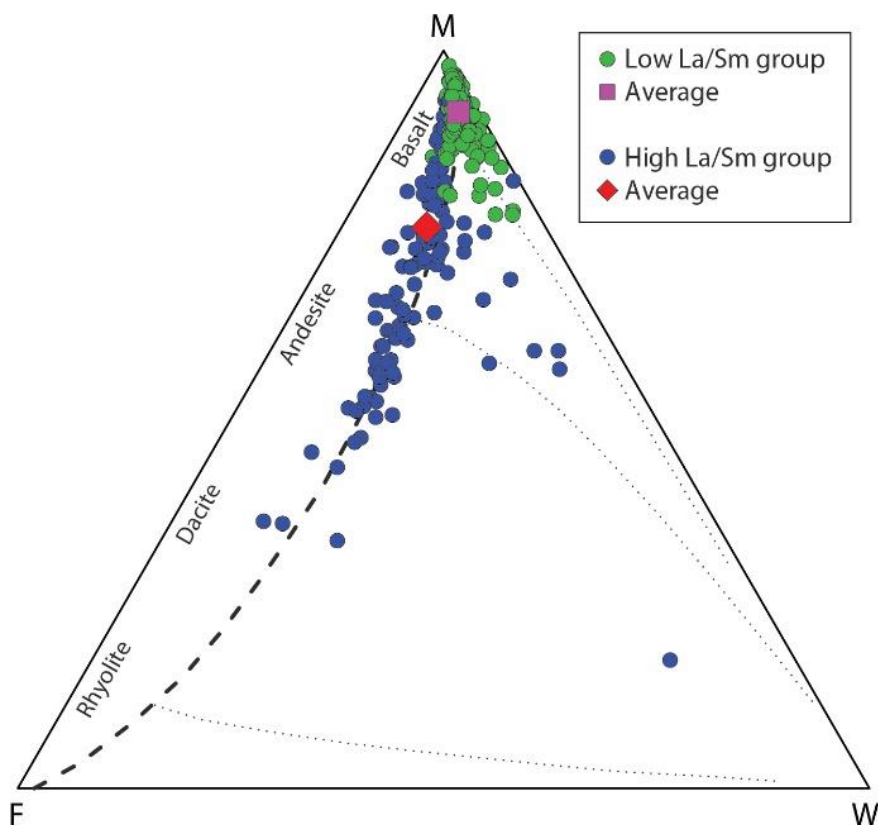


**Figure A6.** Weathering index (W) and the igneous trend from mafic (M) to felsic (F) volcanic rocks [64]. Most of the mid-Archaeon metavolcanic rocks from southwest Greenland plot along the igneous fractionation line, although some samples appear to be overprinted. The shift off the igneous trend can be the result of sedimentary reworking of volcanoclastic deposits, hydrothermal alteration, or perhaps melt modification during metamorphism.

## References

1. Polat, A.; Hofmann, A.W. Alteration and geochemical patterns in the 3.7–3.8 Ga Isua greenstone belt, West Greenland. *Precambrian Res.* **2003**, *126*, 197–218. [\[CrossRef\]](#)
2. Szilas, K.; Hoffmann, J.E.; Münker, C.; Dziggel, A.; Rosing, M.T. Eoarchean within-plate basalts from southwest Greenland: Comment. *Geology* **2014**, *42*, e330. [\[CrossRef\]](#)
3. Bédard, J.H. Stagnant lids and mantle overturns: Implications for Archaean tectonics, magmagenesis, crustal growth, mantle evolution, and the start of plate tectonics. *Geosci. Front.* **2018**, *9*, 19–49. [\[CrossRef\]](#)
4. Wyman, D. Do cratons preserve evidence of stagnant lid tectonics? *Geosci. Front.* **2018**, *9*, 3–17. [\[CrossRef\]](#)
5. Windley, B.F.; Garde, A.A. Arc-generated blocks with crustal sections in the North Atlantic craton of West Greenland: Crustal growth in the Archean with modern analogues. *Earth-Sci. Rev.* **2009**, *93*, 1–30. [\[CrossRef\]](#)
6. Polat, A.; Appel, P.W.; Fryer, B.J. An overview of the geochemistry of Eoarchean to Mesoarchean ultramafic to mafic volcanic rocks, SW Greenland: Implications for mantle depletion and petrogenetic processes at subduction zones in the early Earth. *Gondwana Res.* **2011**, *20*, 255–283. [\[CrossRef\]](#)
7. Polat, A.; Wang, L.; Appel, P.W. A review of structural patterns and melting processes in the Archean craton of West Greenland: Evidence for crustal growth at convergent plate margins as opposed to non-uniformitarian models. *Tectonophysics* **2015**, *662*, 67–94. [\[CrossRef\]](#)
8. Thirlwall, M.F.; Smith, T.E.; Graham, A.M.; Theodorou, N.; Hollings, P.; Davidson, J.P.; Arculus, R.J. High field strength element anomalies in arc lavas: Source or process? *J. Petrol.* **1994**, *35*, 819–838. [\[CrossRef\]](#)
9. Kisters, A.F.; van Hinsberg, V.J.; Szilas, K. Geology of an Archaean accretionary complex—The structural record of burial and return flow in the Tartoq Group of South West Greenland. *Precambrian Res.* **2012**, *220*, 107–122. [\[CrossRef\]](#)
10. Polat, A.; Kokfelt, T.; Burke, K.C.; Kusky, T.M.; Bradley, D.C.; Dziggel, A.; Kolb, J. Lithological, structural, and geochemical characteristics of the Mesoarchean Tartoq greenstone belt, southern West Greenland, and the Chugach–Prince William accretionary complex, southern Alaska: Evidence for uniformitarian plate-tectonic processes. *Can. J. Earth Sci.* **2016**, *53*, 1336–1371. [\[CrossRef\]](#)
11. Dziggel, A.; Diener, J.F.A.; Kolb, J.; Kokfelt, T.F. Metamorphic record of accretionary processes during the Neoarchean: The Nuuk region, southern West Greenland. *Precambrian Res.* **2014**, *242*, 22–38. [\[CrossRef\]](#)
12. Dyck, B.; Reno, B.L.; Kokfelt, T.F. The Majorqaaq Belt: A record of Neoarchean orogenesis during final assembly of the North Atlantic Craton, southern West Greenland. *Lithos* **2015**, *220*, 253–271. [\[CrossRef\]](#)
13. Polat, A.; Frei, R.; Fryer, B.; Appel, P.W. The origin of geochemical trends and Eoarchean (ca. 3700 Ma) zircons in Mesoarchean (ca. 3075 Ma) ocelli-hosting pillow basalts, Ivisartaq greenstone belt, SW Greenland: Evidence for crustal contamination versus crustal recycling. *Chem. Geol.* **2009**, *268*, 248–271. [\[CrossRef\]](#)
14. Zhang, H.F.; Sun, M.; Zhou, X.H.; Zhou, M.F.; Fan, W.M.; Zheng, J.P. Secular evolution of the lithosphere beneath the eastern North China Craton: Evidence from Mesozoic basalts and high-Mg andesites. *Geochim. Cosmochim. Acta* **2003**, *67*, 4373–4387. [\[CrossRef\]](#)
15. Wang, Z.; Wilde, S.A.; Wang, K.; Yu, L. A MORB-arc basalt-adakite association in the 2.5 Ga Wutai greenstone belt: Late Archean magmatism and crustal growth in the North China Craton. *Precambrian Res.* **2004**, *131*, 323–343. [\[CrossRef\]](#)
16. Barley, M.E.; Loader, S.E.; McNaughton, N.J. 3430 to 3417 Ma calc-alkaline volcanism in the McPhee Dome and Kelly Belt, and growth of the eastern Pilbara Craton. *Precambrian Res.* **1998**, *88*, 3–23. [\[CrossRef\]](#)
17. Morris, P.A.; Kirkland, C.L. Melting of a subduction-modified mantle source: A case study from the Archean Marda Volcanic Complex, central Yilgarn Craton, Western Australia. *Lithos* **2014**, *190*, 403–419. [\[CrossRef\]](#)
18. Leclerc, F.; Bédard, J.H.; Harris, L.B.; McNicoll, V.J.; Goulet, N.; Roy, P.; Houle, P. Tholeiitic to calc-alkaline cyclic volcanism in the Roy Group, Chibougamau area, Abitibi Greenstone Belt—Revised stratigraphy and implications for VHMS exploration. *Can. J. Earth Sci.* **2011**, *48*, 661–694. [\[CrossRef\]](#)
19. Lodge, R.W. Petrogenesis of intermediate volcanic assemblages from the Shebandowan greenstone belt, Superior Province: Evidence for subduction during the Neoarchean. *Precambrian Res.* **2016**, *272*, 150–167. [\[CrossRef\]](#)
20. Bédard, J.H. A procedure for calculating the equilibrium distribution of trace elements among the minerals of cumulate rocks, and the concentration of trace elements in the coexisting liquids. *Chem. Geol.* **1994**, *118*, 143–153. [\[CrossRef\]](#)



21. Szilas, K.; van Hinsberg, V.J.; Creaser, R.A.; Kisters, A.F. The geochemical composition of serpentinites in the Mesoarchaeon Tartoq Group, SW Greenland: Harzburgitic cumulates or melt-modified mantle? *Lithos* **2014**, *198*, 103–116. [[CrossRef](#)]
22. Szilas, K.; Kelemen, P.B.; Rosing, M.T. The petrogenesis of ultramafic rocks in the >3.7 Ga Isua supracrustal belt, southern West Greenland: Geochemical evidence for two distinct magmatic cumulate trends. *Gondwana Res.* **2015**, *28*, 565–580. [[CrossRef](#)]
23. Polat, A.; Appel, P.W.; Frei, R.; Pan, Y.; Dilek, Y.; Ordóñez-Calderón, J.C.; Fryer, B.; Hollis, J.A.; Raith, J.G. Field and geochemical characteristics of the Mesoarchean (~3075 Ma) Ivisaartoq greenstone belt, southern West Greenland: Evidence for seafloor hydrothermal alteration in supra-subduction oceanic crust. *Gondwana Res.* **2007**, *11*, 69–91. [[CrossRef](#)]
24. Ordóñez-Calderón, J.C.; Polat, A.; Fryer, B.J.; Appel, P.W.U.; van Gool, J.A.M.; Dilek, Y.; Gagnon, J.E. Geochemistry and geodynamic origin of the Mesoarchean Ujarassuit and Ivisaartoq greenstone belts, SW Greenland. *Lithos* **2009**, *113*, 133–157. [[CrossRef](#)]
25. Szilas, K.; Hoffmann, J.E.; Schulz, T.; Hansmeier, C.; Polat, A.; Viehmann, S.; Kasper, H.U.; Münker, C. Combined bulk-rock Hf-and Nd-isotope compositions of Mesoarchaeon metavolcanic rocks from the Ivisaartoq Supracrustal Belt, SW Greenland: Deviations from the mantle array caused by crustal recycling. *Chem. Erde-Geochem.* **2016**, *76*, 543–554. [[CrossRef](#)]
26. Garde, A.A. A mid-Archaeon island arc complex in the eastern Akia terrane, Godthåbsfjord, southern West Greenland. *J. Geol. Soc.* **2007**, *164*, 565–579. [[CrossRef](#)]
27. Szilas, K.; Tusch, J.; Hoffmann, J.E.; Garde, A.A.; Münker, C. Hafnium isotope constraints on the origin of Mesoarchaeon andesites in southern West Greenland, North Atlantic craton. *Geol. Soc. Lond. Spec. Publ.* **2017**, *449*, 19–38. [[CrossRef](#)]
28. Szilas, K.; Tusch, J.; van Gool, J.A.M.; Münker, C. Andesites of the mid-Archaeon Bjørneøen Supracrustal Belt, SW Greenland: Evidence for Archaeon subduction zone? *Precambrian Res.* **2018**, under review.
29. Szilas, K.; van Gool, J.A.; Scherstén, A.; Frei, R. The Neoarchaeon Storø Supracrustal Belt, Nuuk region, southern West Greenland: An arc-related basin with continent-derived sedimentation. *Precambrian Res.* **2014**, *247*, 208–222. [[CrossRef](#)]
30. Szilas, K.; Garde, A.A. Mesoarchaeon aluminous rocks at Storø, southern West Greenland: New age data and evidence of premetamorphic seafloor weathering of basalts. *Chem. Geol.* **2013**, *354*, 124–138. [[CrossRef](#)]
31. Szilas, K.; Maher, K.; Bird, D.K. Aluminous gneiss derived by weathering of basaltic source rocks in the Neoarchaeon Storø Supracrustal Belt, southern West Greenland. *Chem. Geol.* **2016**, *441*, 63–80. [[CrossRef](#)]
32. Szilas, K.; Hoffmann, J.E.; Hansmeier, C.; Hollis, J.A.; Münker, C.; Viehmann, S.; Kasper, H.U. Sm-Nd and Lu-Hf isotope and trace-element systematics of Mesoarchaeon amphibolites, inner Ameralik fjord, southern West Greenland. *Mineral. Mag.* **2015**, *79*, 857–876. [[CrossRef](#)]
33. Szilas, K.; Næraa, T.; Scherstén, A.; Stendal, H.; Frei, R.; van Hinsberg, V.J.; Kokfelt, T.F.; Rosing, M.T. Origin of Mesoarchaeon arc-related rocks with boninite/komatiite affinities from southern West Greenland. *Lithos* **2012**, *144*, 24–39. [[CrossRef](#)]
34. Szilas, K.; Hoffmann, J.E.; Scherstén, A.; Kokfelt, T.F.; Münker, C. Archaeon andesite petrogenesis: Insights from the Grædefjord Supracrustal Belt, southern West Greenland. *Precambrian Res.* **2013**, *236*, 1–15. [[CrossRef](#)]
35. Szilas, K.; Hoffmann, J.E.; Scherstén, A.; Rosing, M.T.; Windley, B.F.; Kokfelt, T.F.; Keulen, N.; van Hinsberg, V.J.; Næraa, T.; Frei, R.; et al. Complex calc-alkaline volcanism recorded in Mesoarchaeon supracrustal belts north of Frederikshåb Isblink, southern West Greenland: Implications for subduction zone processes in the early Earth. *Precambrian Res.* **2012**, *208*, 90–123. [[CrossRef](#)]
36. Klausen, M.B.; Szilas, K.; Kokfelt, T.F.; Keulen, N.; Schumacher, J.C.; Berger, A. Tholeiitic to calc-alkaline metavolcanic transition in the Archean Nigerlikasik Supracrustal Belt, SW Greenland. *Precambrian Res.* **2017**, *302*, 50–73. [[CrossRef](#)]
37. Szilas, K.; van Hinsberg, V.J.; Kisters, A.F.; Hoffmann, J.E.; Windley, B.F.; Kokfelt, T.F.; Scherstén, A.; Frei, R.; Rosing, M.T.; Münker, C. Remnants of arc-related Mesoarchaeon oceanic crust in the Tartoq Group of SW Greenland. *Gondwana Res.* **2013**, *23*, 436–451. [[CrossRef](#)]
38. Janoušek, V.; Farrow, C.M.; Erban, V. Interpretation of whole-rock geochemical data in igneous geochemistry: Introducing Geochemical Data Toolkit (GCDkit). *J. Petrol.* **2006**, *47*, 1255–1259. [[CrossRef](#)]
39. Irvine, T.N.; Baragar, W.R.A. A guide to the chemical classification of the common volcanic rocks. *Can. J. Earth Sci.* **1971**, *8*, 523–548. [[CrossRef](#)]

40. Pearce, J.A. A User's Guide to Basalt Discrimination Diagrams. In *Trace Element Geochemistry of Volcanic Rocks: Applications for Massive Sulphide Exploration*; Wyman, D.A., Ed.; Short Course Notes; Geological Association of Canada: St. John's, NL, Canada, 1996; Volume 12, pp. 79–113.
41. Palme, H.; O'Neill, H.S.C. Composition of the Primitive Mantle. In *Treatise on Geochemistry*, 2nd ed.; Holland, H.D., Turekian, K., Eds.; Elsevier Science: Amsterdam, The Netherlands, 2003; pp. 1–38.
42. Arndt, N.T. High Ni in Archean tholeiites. *Tectonophysics* **1991**, *187*, 411–419. [[CrossRef](#)]
43. Kerrich, R.; Polat, A.; Wyman, D.; Hollings, P. Trace element systematics of Mg-, to Fe-tholeiitic basalt suites of the Superior Province: Implications for Archean mantle reservoirs and greenstone belt genesis. *Lithos* **1999**, *46*, 163–187. [[CrossRef](#)]
44. Baier, J.; Audétat, A.; Keppler, H. The origin of the negative niobium tantalum anomaly in subduction zone magmas. *Earth Planet. Sci. Lett.* **2008**, *267*, 290–300. [[CrossRef](#)]
45. Kelemen, P.B.; Hanghøj, K.; Greene, A.R. One view of the geochemistry of subduction-related magmatic arcs, with an emphasis on primitive andesite and lower crust. *Treatise Geochem.* **2003**, *3*, 659. [[CrossRef](#)]
46. Nicholls, I.A.; Harris, K.L. Experimental rare earth element partition coefficients for garnet, clinopyroxene and amphibole coexisting with andesitic and basaltic liquids. *Geochim. Cosmochim. Acta* **1980**, *44*, 287–308. [[CrossRef](#)]
47. Grove, T.L.; Kinzler, R.J. Petrogenesis of andesites. *Annu. Rev. Earth Planet. Sci.* **1986**, *14*, 417–454. [[CrossRef](#)]
48. Kelemen, P.B. Genesis of high Mg# andesites and the continental crust. *Contrib. Mineral. Petrol.* **1995**, *120*, 1–19.
49. Reubi, O.; Blundy, J. A dearth of intermediate melts at subduction zone volcanoes and the petrogenesis of arc andesites. *Nature* **2009**, *461*, 1269–1273. [[CrossRef](#)] [[PubMed](#)]
50. Li, C.; Arndt, N.T.; Tang, Q.; Ripley, E.M. Trace element indiscrimination diagrams. *Lithos* **2015**, *232*, 76–83. [[CrossRef](#)]
51. Hollocher, K.; Robinson, P.; Walsh, E.; Roberts, D. Geochemistry of amphibolite-facies volcanics and gabbros of the Støren Nappe in extensions west and southwest of Trondheim, Western Gneiss Region, Norway: A key to correlations and paleotectonic settings. *Am. J. Sci.* **2012**, *312*, 357–416. [[CrossRef](#)]
52. Pearce, J.A. Geochemical fingerprinting of oceanic basalts with applications to ophiolite classification and the search for Archean oceanic crust. *Lithos* **2008**, *100*, 14–48. [[CrossRef](#)]
53. Bédard, J.H. How many arcs can dance on the head of a plume? A 'Comment' on: A critical assessment of Neoarchean 'plume only' geodynamics: Evidence from the Superior province, by Derek Wyman, Precambrian Research, 2012. *Precambrian Res.* **2013**, *229*, 189–197. [[CrossRef](#)]
54. Spera, F.J.; Bohrsen, W.A. Energy-constrained open-system magmatic processes I: General model and energy-constrained assimilation and fractional crystallization (EC-AFC) formulation. *J. Petrol.* **2001**, *42*, 999–1018. [[CrossRef](#)]
55. Kovalenko, A.; Clemens, J.D.; Savatenkov, V. Petrogenetic constraints for the genesis of Archean sanukitoid suites: Geochemistry and isotopic evidence from Karelia, Baltic Shield. *Lithos* **2005**, *79*, 147–160. [[CrossRef](#)]
56. Bédard, J.H.; Harris, L.B.; Thurston, P.C. The hunting of the snArc. *Precambrian Res.* **2013**, *229*, 20–48. [[CrossRef](#)]
57. Barnes, S.J.; Van Kranendonk, M.J. Archean andesites in the east Yilgarn craton, Australia: Products of plume-crust interaction? *Lithosphere* **2014**, *6*, 80–92. [[CrossRef](#)]
58. Anders, E.; Grevesse, N. Abundances of the elements: Meteoritic and solar. *Geochim. Cosmochim. Acta* **1989**, *53*, 197–214. [[CrossRef](#)]
59. Jensen, L.S. *A New Cation Plot for Classifying Subalkalic Volcanic Rocks*; Miscellaneous Paper 66; Ministry of Natural Resources: Peterborough, ON, Canada, 1976.
60. Miyashiro, A. Volcanic rock series in island arcs and active continental margins. *Am. J. Sci.* **1974**, *274*, 321–355. [[CrossRef](#)]
61. Middlemost, E.A. Naming materials in the magma/igneous rock system. *Earth-Sci. Rev.* **1994**, *37*, 215–224. [[CrossRef](#)]
62. Shand, S.J. *Eruptive Rocks. Their Genesis, Composition, Classification, and Their Relation to Ore-Deposits with a Chapter on Meteorite*; John Wiley & Sons: New York, NY, USA, 1943.

63. Pearce, J.A.; Cann, J.R. Tectonic setting of basic volcanic rocks determined using trace element analyses. *Earth Planet. Sci. Lett.* **1973**, *19*, 290–300. [[CrossRef](#)]
64. Ohta, T.; Arai, H. Statistical empirical index of chemical weathering in igneous rocks: A new tool for evaluating the degree of weathering. *Chem. Geol.* **2007**, *240*, 280–297. [[CrossRef](#)]



© 2018 by the author. Licensee MDPI, Basel, Switzerland. This article is an open access article distributed under the terms and conditions of the Creative Commons Attribution (CC BY) license (<http://creativecommons.org/licenses/by/4.0/>).